Korean J. Chem. Eng., 39(12), 3261-3266 (2022)
DOI: 10.1007/s11814-022-1214-0

pISSN: 0256-1115
eISSN: 1975-7220

Acoustic bubble array-induced jet flow for cleaning particulate contaminants on semiconductor wafers

Daegeun Kim*, Jiwoo Hong,†, and Sang Kug Chung*,†**

*Department of Mechanical Engineering, Myongji University, 116, Myongji-ro, Cheoin-gu, Yongin-si, Gyeonggido 17058, Korea
**School of Mechanical Engineering, Soongsil University, 369 Sangdo-ro, Dongjak-gu, Seoul 06978, Korea
(*Received 1 June 2022 • Revised 21 June 2022 • Accepted 25 June 2022*)

Abstract−The demand for semiconductors and the necessity of developing the next-generation semiconductor have skyrocketed with recent technological advancements, such as next-generation mobile networks, cloud computing, the Internet of Things, and artificial intelligence. Accordingly, a new type of semiconductor cleaning technique that can minimize environmental impact and physical harm to the exceedingly thin structures in semiconductor chips must be developed. This work proposes a cleaning strategy for particle contamination on semiconductor wafer surfaces by utilizing jet flow created by bubble oscillation constrained in arrays of microcylinders. The variation in the maximum jet flow velocity caused by single bubble oscillation constrained in a microcylinder, which is affected by physical factors, such as applied voltage, frequency, and microcylinder dimensions, has been investigated. A wafer cleaning apparatus that comprised 9×9 arrays of microcylinders was designed based on experimental data on single bubble oscillation constrained in a microcylinder. The maximum jet flow velocity for the multi-arrays of microcylinders can be attained up to 148.5 mm/s, which is nearly five times the maximum value obtained from a single cylinder, even with a lower voltage applied than with a single microcylinder. The wafer cleaning apparatus removes particulates with different wettabilities and sizes from contaminated semiconductor wafers successfully with a high cleaning efficiency of up to 92.5%. The current effort makes an important contribution to the development of semiconductor cleaning techniques that can meet the requirements of current and next-generation semiconductor manufacturing in terms of yield, stability, and environmental pollution.

Keywords: Bubble Oscillation, Microstreaming Flow, Semiconductor Cleaning Technique

INTRODUCTION

Semiconductors have become ubiquitous because of the rapid development of cutting-edge technology, such as next-generation mobile networks, the Internet of Things, and artificial intelligence. With the high demand for current semiconductors and the need for next-generation semiconductors on an extremely small scale, the role of cleaning technology that removes undesired particulate contaminants (e.g., particles and metal debris) on the semiconductor wafer, which has a significant negative impact on semiconductor yield and reliability, has been enhanced [1-3].

Depending on the size of the particulate contaminants, conventional cleaning techniques for semiconductors, such as brush [4,5], ultrasonic [6,7], and electrochemical cleaning with an ammonium peroxide mixture (APM) [2,8], have been widely used. Brushing or high-intensity ultrasonic waves can damage the micro/nano patterns (or structures) on the semiconductor wafer physically, or the APM can etch the patterns away during the cleaning process chemically, thereby affecting semiconductor yield and reliability [9-11]. Thus, developing an alternative semiconductor cleaning process that can remove particulate impurities effectively without disrupting the patterns or structures on the semiconductor surface is critical. We would like to begin by noting bubble oscillation as a potential clue for developing new semiconductor cleaning techniques.

Bubble oscillation induced by external excitations, such as acoustic, electrical, and mechanical vibration, is a fascinating and practical topic in academic and industrial domains [12-15]. In particular, the intriguing fluid dynamic phenomena [13,14] caused by oscillating bubbles, such as secondary sound field and streaming flow, have raised the bubble's importance and applicability in the microfluidic research area to new heights. Many researchers have developed a wide range of microfluidic techniques, such as fluidic regulators [16-19] and micro-object manipulators [20-26], as well as engineering (particularly biochemical or biomedical) applications [27-31] by utilizing oscillating bubbles and the resulting fluidic phenomena. A few recently published review papers provided concise summaries of bubble oscillation-based microfluidic applications [15,32-34].

In this work, we suggest a cleaning technique for particle contamination on semiconductor wafer surfaces by drawing inspiration from remarkable fluid dynamic phenomena, including the synthetic jet flow caused by oscillating bubbles. Fig. 1 illustrates the proposed jet flow-assisted cleaning apparatus conceptually. This apparatus is constructed mostly from arrays of microcylinders and a piezoactuator. When the arrays of microcylinders in the cleaning device are immersed in chemical solution or distilled water, bubbles are

†To whom correspondence should be addressed.
E-mail: jiwoohong@ssu.ac.kr, skchung@mju.ac.kr

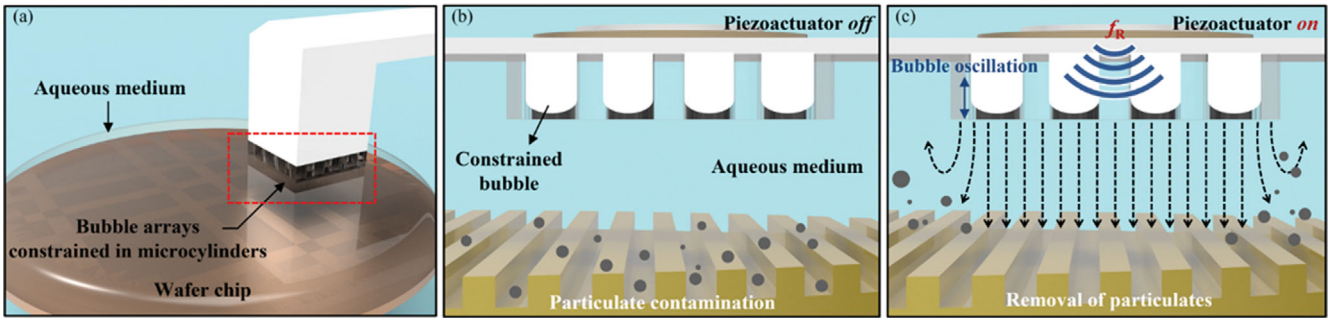

Fig. 1. Conceptual diagram of the proposed jet flow-assisted cleaning technology. (a) A wafer cleaning system comprised of arrays of oscillating bubbles contained within microcylinders. (b) Jet flow-assisted cleaning device with bubble arrays is placed near contaminated semiconductor wafer surfaces. (c) When a piezoactuator attached to the device is activated, the bubbles acoustically oscillate, thereby generating synthetic jets that remove particulate contaminants from semiconductor wafer surfaces.

naturally trapped inside the hydrophobic-treated microcylinders. When confined bubbles in microcylinders are actuated acoustically by a piezoactuator, they oscillate and generate synthetic jets that clean particulate contaminants, such as dust and debris from nano/micropatterned areas on semiconductor chips.

To demonstrate the feasibility of the suggested cleaning technology, we preferentially explore jet flow characteristics induced by single bubble oscillation constrained in a microcylinder and the physical factors that control them, such as applied voltage, frequency, and microcylinder dimensions. We constructed a wafer cleaning equipment composed of several arrays of microcylinders and tested its cleaning performance under simulated particulate contamination on semiconductor wafer surfaces.

EXPERIMENTAL DETAILS

Fig. 2 depicts the fabrication procedure of the proposed wafer cleaning device, which is primarily composed of an array of oscillating bubbles subjected to acoustic excitation, as well as the entire experimental setup for the wafer cleaning technique. As shown in Fig. 2(a), the arrays of microcylinders with a reverse conical shape and one end open are microfabricated onto an acrylic block using a laser lithography method, similar to previous works [35,36]. Following that, the inner walls of the microcylinders are deposited with parylene using a chemical vapor deposition process to produce hydrophobic surfaces, hence allowing bubbles to be spontaneously trapped to the microcylinders as the device is submerged in water. Finally, the top side of the chip is glued with UV epoxy to a disk-type piezoactuator (MFT-27T-4.1A1, KEPO Co.). The fabricated wafer cleaning device, which consists of 9×9 square arrays of microcylinders with dimensions in 10×10 cm^2, is shown in Fig. 2(b). The microcylinders all have a diameter of 100 μm and a length of 5 mm. When the microcylinder arrays are submerged, the created bubbles have nearly the same diameter and length as the micro-

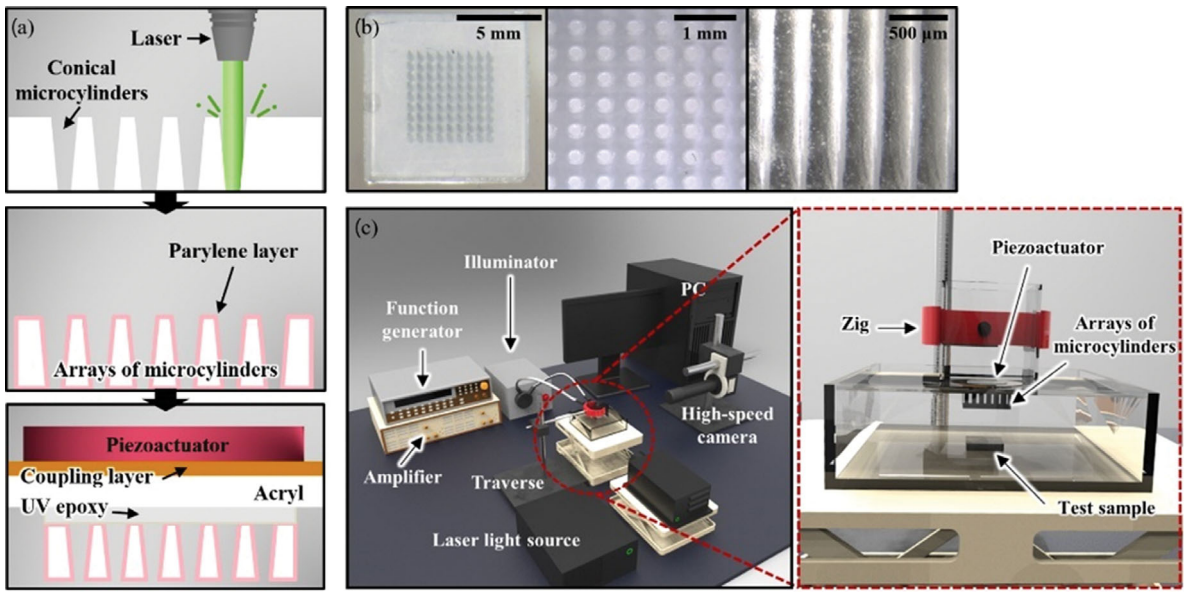

Fig. 2. Schematic of (a) the fabrication procedure of the proposed wafer cleaning device, which is primarily composed of an array of oscillating bubbles subjected to acoustic excitation. (b) Fabricated arrays of microcylinders for bubble trapping. (c) Entire experimental setup for a wafer cleaning technique based on the acoustic excitation of confined bubble arrays.

cylinders.

A top-open water chamber (dimensions in 6.5×6.5×4.5 cm^3) was constructed with transparent acrylic plates for the visualization of bubble motion and it-induced external flow. To excite the constrained bubbles inside the arrays of microcylinders acoustically, electrical signals generated by a function generator (33210A, Agilent Co.) and amplified (PZD700, Trek Co.) are applied to the piezoactuator. The dynamic behavior of the acoustically oscillating bubbles and the external flows that surround them was recorded sequentially using a high-speed camera (Phantom Miro eX4, Vision Research Inc.) integrated with a zoom lens (VZMTM 450i eo, Edmund Optics). The particle image velocimetry (PIV) technique with the illumination of a continuous laser (PSUH-LED, Changchun New Industries Optoelectronics Tech. Co. Ltd.) and the seeding of micro-fluorescent particles (6 μm in a diameter, Duke Scientific Corp.), as well as conventional PIV software (INSIGHT 4G, TSI Incorporated), were used to obtain quantitative information on the external flows.

To simulate a scenario of particulate contamination on a semiconductor, microparticles are coated on patterned silicon wafers through spin coating. The patterned silicon wafers are fabricated using conventional photolithography techniques, such as photoresist deposition, UV exposure, and developing. Hydrophobic microparticles (silica particle, 5-15 μm in diameter) and hydrophilic microparticles (carboxy-modified acrylate-based polymer particle, 6 μm and 15 μm in diameter) are utilized in this study to compare and analyze the cleaning efficiency of the proposed cleaning technique according to particle wettability and size. The number of microparticles on the wafer is estimated before and after cleaning by using a metallurgical microscope (GX51, OLYMPUS) and particle counting function of an image analyzer (ImageJ, NIH, Bethesda, ML). Every experiment was carried out at least five times, and the data presented in the Results and Discussion section are the average of the results.

RESULTS AND DISCUSSION

To obtain fundamental information for developing our proposed cleaning technology, we preferentially observed and analyzed jet flow features induced by single bubble oscillation constrained in a microfabricated microcylinder using high-speed imaging and micro-PIV techniques over a wide range of applied voltage and frequency. As shown in Fig. 3(a), a very violent jet flow is observed around an oscillation constrained in microcylinder at a specific frequency. The resonance frequency can be determined experimentally by locating the specific frequency in the present work. Furthermore, information about the jet flow fields, especially velocity amplitude, can be extracted from high-speed images using conventional PIV software Fig. 3(b). Fluidic information of synthetic jet flow, such as maximum velocity and resonance frequency, can be obtained using flow visualization and PIV measurements to evaluate the physical factors that influence cleaning efficiency (e.g., applied voltage and frequency, bubble dimensions, and distance from wafer sample) in developing our proposed cleaning technique.

The oscillation amplitude of the constrained bubble in the microcylinder, which is well known to be greatest at the resonance frequency, can be expected to influence the velocity of the jet flow. To understand the relationship between the maximum jet flow velocity and applied frequency, the maximum velocity is measured by varying applied frequency at a fixed applied voltage of 500 V_{pp} (Fig. 4(a)). The maximum jet flow velocity is greatest when the applied frequency is 1.87 kHz, which is identified as the empirically determined resonance frequency. Here, the dimensionless applied frequency is defined as the applied frequency divided by the resonance frequency of the oscillating constrained bubble. The dimensionless applied frequency has a value of one, which indicates that the applied frequency corresponds to the resonance frequency.

We also investigated the variation of the maximum jet flow velocity with respect to applied voltage at various applied frequencies (Fig. 4(b)). Regardless of the applied frequency, the maximum jet flow velocity tends to increase in general as applied voltage rises. When a voltage larger than 500 V_{pp} is applied to boost the maximum jet flow rate, the constrained bubble is witnessed to vibrate violently and eventually escape. A systematical examination of the geometry or wettability of the microcylinder, which can strongly confine the oscillation bubble even at high voltage, will be conducted to boost the maximum jet flow rate. Furthermore, the minimum applied voltage necessary to generate jet flow increases with the dimensionless applied frequency (i.e., the disparity between the applied and resonance frequencies).

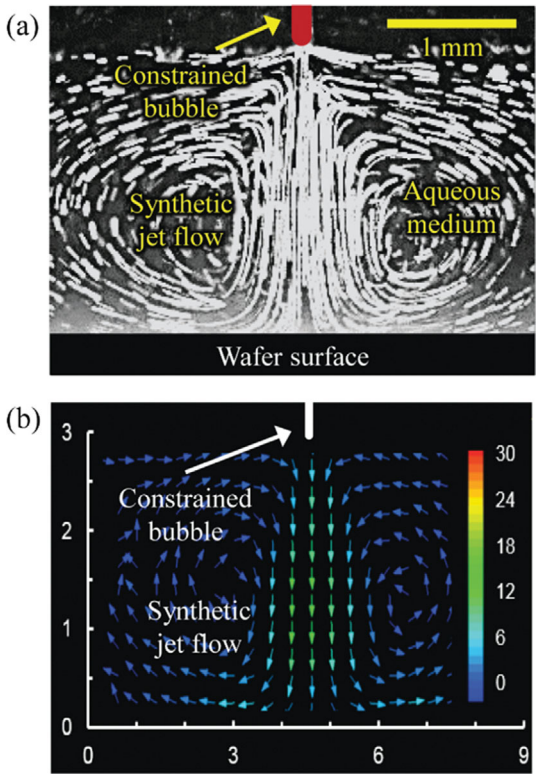

Fig. 3. (a) Flow visualization and (b) particle image velocimetry (PIV) measurements of the flow field that surrounds an oscillating bubble constrained in a microcylinder. Here, the values of the applied voltage and frequency are 350 V_{pp} and 1.87 kHz, respectively. The legend bar in Fig. 2(b) represents the velocity amplitude of jet flow in millimeters per second.

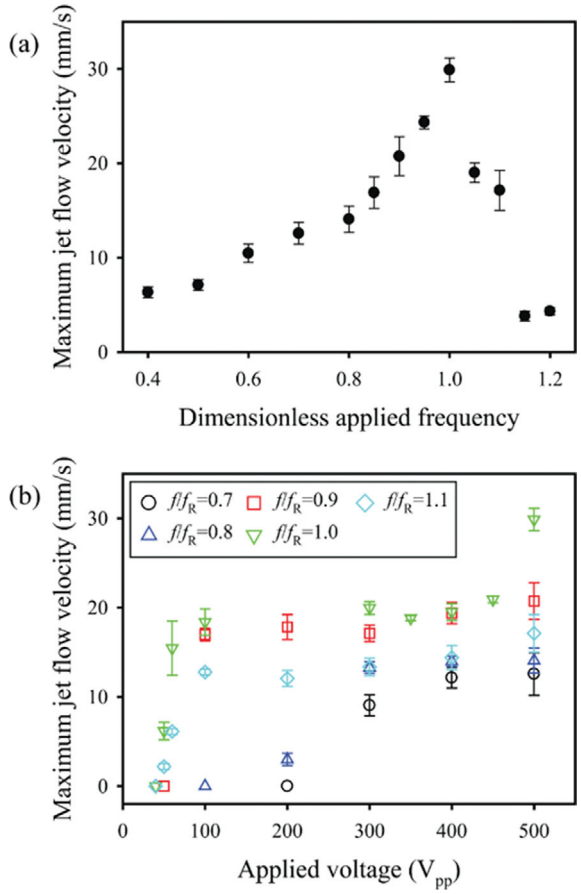

Fig. 4. (a) Maximum jet flow velocity induced by the oscillation of a constrained bubble as a function of dimensionless applied frequency at a fixed voltage of 500 V_{pp}. Here, the dimensionless applied frequency is defined as the applied frequency divided by the resonance frequency of the oscillating bubble. (b) Maximum jet flow velocity as a function of applied voltage and frequency.

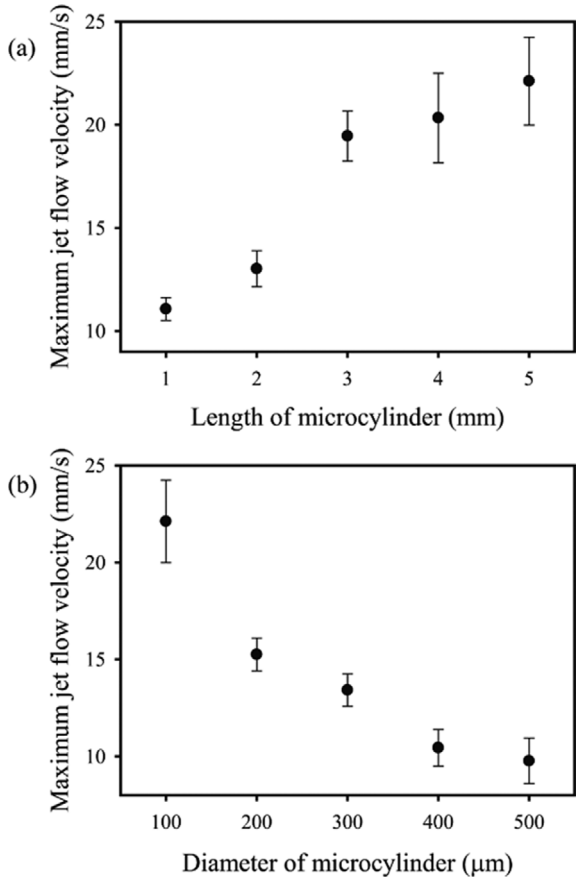

Fig. 5. Maximum jet flow velocity as a function of (a) length and (b) diameter of microcylinder. In this work, the applied voltage was set to 100 V_{pp}, and the applied frequency was set to match the resonance frequency determined experimentally for each bubble dimension.

The bubble dimensions (e.g., diameter, length) could be a physical factor that influences bubble oscillation and resulting jet flow velocity. To verify this, the variance in the maximum jet flow velocity was quantified using oscillating bubbles contained in microcylinders of varying lengths and diameters (Fig. 5). The dimensions of the bubble are considered the same as those of the microcylinder. Here, the applied voltage was set to 100 V_{pp}, and the applied frequency is set to match the resonance frequency determined experimentally for each bubble dimension. The maximum jet flow velocity increases as the length of the microcylinder (or constrained bubble) increases, with a fixed diameter of 100 μm for the microcylinder (Fig. 5(a)). In contrast, at a fixed length of 5 mm for the microcylinder (or constrained bubble), the maximum jet flow velocity decreases as the microcylinder diameter increases (Fig. 5(b)). It is known that the maximum jet flow velocity increases linearly with the amplitude and resonance frequency of the confined bubble oscillation [36-38]. The resonance frequency, on the other hand, is known to be inversely proportional to the square root of the length and diameter of the microcylinder [37]. Although the resonance frequency decreases as the length and diameter of the microcylinder increase, the tendencies shown in Fig. 5 may be attributed to an increase in oscillation amplitude as these dimensions increase.

Based on the fundamental information presented above about the oscillation of a single confined bubble and its induced jet flow, a wafer cleaning apparatus that consists of 9×9 arrays of microcylinders was devised. To determine an optimal distance condition for improving cleaning efficiency preferentially, the maximum jet flow velocity was measured by varying the distance between the wafer cleaning device and the sample wafer chip (Fig. 6(a)). The applied voltage and frequency for this experiment were set to 270 V_{pp} and 2.48 kHz, respectively, where the most violent jet flow is experimentally observed. As shown in Fig. 6(a), the maximum jet flow velocity peaks when the cleaning device is 5 mm away from the sample wafer and it then tends to decrease as the distance increases. When 9×9 arrays of microcylinders are used, the maximum jet flow velocity can be attained up to 148.5 mm/s even with a lower voltage applied than with a single cylinder. This is nearly five times the highest value (29.9 mm/s) obtained from a single cylinder.

As described in the Experimental details section, microparticles with different sizes and wettabilities are coated on patterned silicon wafers to simulate the scenarios of particulate contamination on semiconductor wafers. For convenience, hydrophobic silica micro-

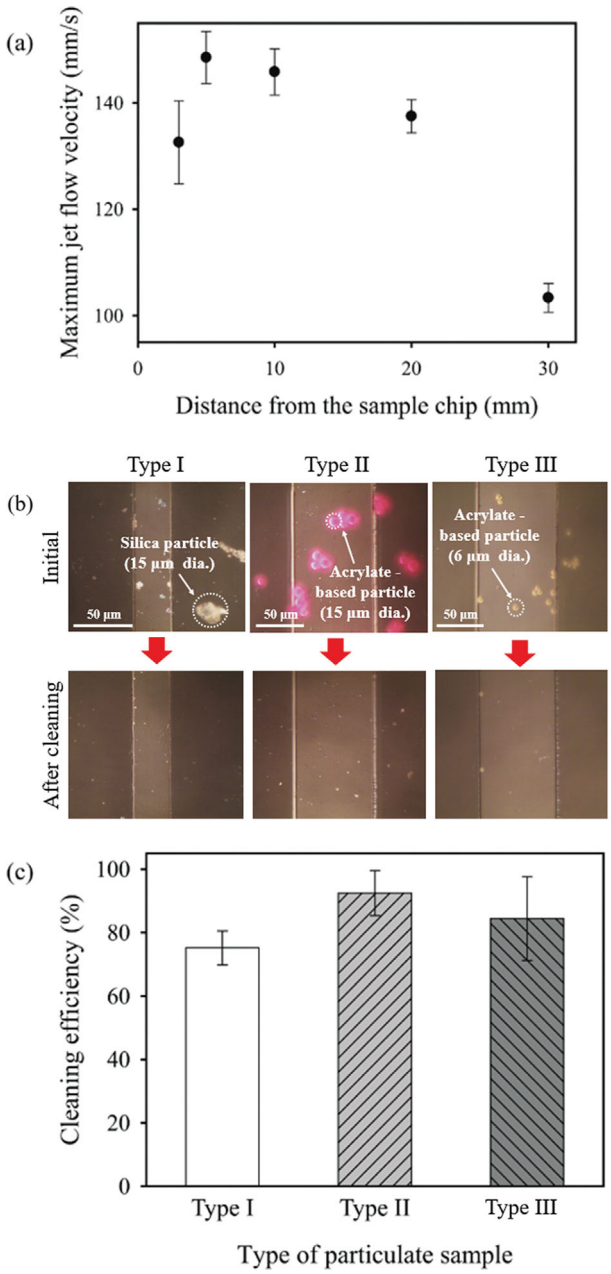

Fig. 6. (a) Maximum jet flow velocity generated by a wafer cleaning apparatus comprised of 9×9 arrays of microcylinders as a function of distance between the wafer cleaning device and the sample wafer chip. (b) Removal of particulate contamination with varying wettability and size from semiconductor wafers using the wafer cleaning apparatus. (c) Cleaning efficiency for different particulate samples. Type I, Type II, and Type III are hydrophobic silica microparticles (5 μm to 15 μm in diameter) and hydrophilic acrylate-based microparticles (15 μm and 6 μm in diameter).

particles (5-15 μm in diameter) and hydrophilic acrylate-based microparticles with 15 μm and 6 μm in diameter are referred to as Type I, Type II, and Type III, respectively. The patterned substrate polluted with the microparticles can be cleaned by performing jet flow-based cleaning for 3 minutes with a wafer cleaning apparatus (Fig. 6(b)). When the jet flow-based cleaning procedure was performed for 3 minutes using our devised cleaning apparatus, the microparticles of all types were visibly eliminated from the contaminated patterned wafer.

We conducted a quantitative analysis of the cleaning efficiency of the proposed cleaning technique for each type of microparticle (Fig. 6(c)). In this work, cleaning efficiency is defined as the number of microparticles removed following cleaning divided by the number of microparticles present prior to cleaning, expressed as a percentage. Cleaning efficiency for Type I, Type II, and Type III was measured to be 75.2%, 92.5%, and 84.4%, respectively. Hydrophobic particles are removed more efficiently than hydrophilic particles, and larger hydrophobic particles are removed slightly more efficiently than smaller hydrophobic ones. In the future, we will conduct further research on the removal of various contaminants from wafers with various 3D structures using the proposed cleaning technology to come closer to the actual semiconductor cleaning process.

CONCLUSION

By drawing inspiration from intriguing fluid dynamic phenomena, including synthetic jet flow created by oscillating bubbles, we propose a cleaning strategy for particle contamination on semiconductor wafer surfaces. First, we observed and analyzed jet flow characteristics caused by single bubble oscillation constrained in a microfabricated microcylinder over a wide range of applied voltage and frequency with a high-speed micro-PIV technique. The maximum jet flow velocity was discovered to be greatest at the experimentally determined resonance frequency, and it increased as applied voltage increased. In addition, the effects of microcylinder dimensions were investigated as another physical factor that influences bubble oscillation and resulting jet flow velocity. The maximum jet flow velocity was found to increase with increasing microcylinder length and decreasing microcylinder diameter. Based on fundamental information on the oscillation of a single confined bubble and its induced jet flow, we designed and fabricated a wafer cleaning apparatus comprised of 9×9 arrays of microcylinders. To emulate scenarios of particulate contamination on semiconductor wafers, patterned silicon wafers were coated with microparticles of various sizes and wettability. The microparticles can be removed from the contaminated patterned wafer with a high cleaning efficiency of up to 92.5% by using the wafer cleaning apparatus. Finally, in the near future, we will develop a unique cleaning strategy that uses backward microstreaming flow to suck up particulate contaminants from semiconductor wafers by adjusting the position of an acoustically oscillating bubble's gas-liquid interface [39]. The proposed particulate removal strategy, which is based on oscillating bubble-induced jet flow, opens possibilities as an alternative cleaning technology that can alleviate the limitations of existing cleaning technologies by minimizing the use of toxic chemicals and physical damage to fine structures on semiconductor chips.

ACKNOWLEDGEMENTS

This research was supported by Basic Science Research Program through the National Research Foundation of Korea (NRF) funded

by the Ministry of Education (2020R1F1A107488812).

CONFLICT OF INTEREST

The authors declare no conflict of interest.

REFERENCES

1. V. B. Menon, *Particle control for semiconductor manufacturing*, 1st ed., Routledge, London (1990).
2. K. Qin and Y. Li, *J. Colloid Interface Sci.*, **261**, 569 (2003).
3. G. W. Gale, H. Cui and K. A. Reinhardt, *Handbook of silicon wafer cleaning technology*, 3rd ed., William Andrew, New York (2018).
4. D. Hymes, I. Malik, J. Zhang and R. Emami, *Solid State Technol.*, **40**, 209 (1997).
5. K. Xu, R. Vos, G. Vereecke, G. Doumen, W. Fyen, P. W. Mertens, M. M. Heyns, C. Vinckier, J. Fransaer and F. Kovacs, *J. Vac. Sci. Technol. B*, **23**, 2160 (2005).
6. T. Kuehn, D. Kittelson, Y. Wu and R. Gouk, *J. Aerosol. Sci.*, **27**, 427 (1996).
7. G. Gale and A. Busnaina, *Part. Sci. Technol.*, **13**, 197 (1995).
8. K. Yamamoto, A. Nakamura and U. Hase, *IEEE Trans. Semicond. Manuf.*, **12**, 288 (1999).
9. T. Hattori, *Ultraclean surface processing of silicon wafers*, Springer, Heidelberg (1998).
10. X. Li, A. J. Strojwas, A. L. Swecker, M. Reddy, L. Milor and Y. Lin, *Proc. SPIE*, **3216**, 167 (1997).
11. H. F. Okorn-Schmidt, F. Holsteyns, A. Lippert, D. Mui, M. Kawaguchi, C. Lechner, P. E. Frommhold, T. Nowak, F. Reuter, M. B. Piqué, C. Cairós and R. Mettin, *ECS J. Solid State Sci. Technol.*, **3**, N3069 (2013).
12. M. S. Plesset and A. Prosperetti, *Annu. Rev. Fluid Mech.*, **9**, 145 (1977).
13. W. Lauterborn and T. Kurz, *Rep. Prog. Phys.*, **73**, 106501 (2010).
14. A. J. B. Milne, B. Defez, M. Cabrerizo-Vílchez and A. Amirfazli, *Adv. Colloid Interface Sci.*, **203**, 22 (2014).
15. A. Hashmi, G. Yu, M. Reilly-Collette, G. Heiman and J. Xu, *Lab Chip*, **12**, 4216 (2012).
16. K. Ryu, S. K. Chung and S. K. Cho, *J. Assoc. Lab. Autom.*, **15**, 163 (2010).
17. A. R. Tovar, M. V. Patel and A. P. Lee, *Microfluid. Nanofluid.*, **10**, 1269 (2011).
18. M. V. Patel, I. A. Nanayakkara, M. G. Simon and A. P. Lee, *Lab Chip*, **14**, 3860 (2014).
19. R. H. Liu, J. Yang, M. Z. Pindera, M. Athavale and P. Grodzinski, *Lab Chip*, **2**, 151 (2002).
20. S. K. Chung, Y. Zhao and S. K. Cho, *J. Micromech. Microeng.*, **18**, 095009 (2008).
21. S. K. Chung and S. K. Cho, *J. Micromech. Microeng.*, **18**, 125024 (2008).
22. S. K. Chung and S. K. Cho, *Microfluid. Nanofluid.*, **6**, 261 (2009).
23. J. O. Kwon, J. S. Yang, S. J. Lee, K. Rhee and S. K. Chung, *J. Micromech. Microeng.*, **21**, 115023 (2011).
24. S. K. Chung, J. O. Kwon and S. K. Cho, *J. Adhes. Sci. Technol.*, **26**, 1965 (2012).
25. K. H. Lee, J. H. Lee, J. M. Won, K. Rhee and S. K. Chung, *Sens. Actuator A-Phys.*, **188**, 442 (2012).
26. J. H. Shin, J. Seo, J. Hong and S. K. Chung, *Sens. Actuator B-Chem.*, **246**, 415 (2017).
27. Z. Dong, C. Yao, X. Zhang, J. Xu, G. Chen, Y. Zhao and Q. Yuan, *Lab Chip*, **15**, 1145 (2015).
28. Y. Chen and S. Lee, *Integr. Comp. Biol.*, **54**, 959 (2014).
29. J. S. Oh, Y. S. Kwon, K. H. Lee, W. Jeong, S. K. Chung and K. Rhee, *Comput. Biol. Med.*, **44**, 37 (2014).
30. P. Marmottant and S. Hilgenfeldt, *Nature*, **423**, 153 (2003).
31. S. L. Gac, E. Zwaan, A. van den Berg and C.-D. Ohl, *Lab Chip*, **7**, 1666 (2007).
32. S. K. Chung, K. Rhee and S. K. Cho, *Int. J. Precis. Eng. Manuf.*, **11**, 991 (2010).
33. Y. Li, X. Liu, Q. Huang, A. T. Ohta and T. Arai, *Lab Chip*, **21**, 1016 (2021).
34. A. Ozcelik, J. Rich and T. J. Huang, *Lab Chip*, **22**, 297 (2022).
35. J. Feng, J. Yuan and S. K. Cho, *Lab Chip*, **16**, 2317 (2016).
36. J. Feng, J. Yuan and S. K. Cho, *Lab Chip*, **15**, 1554 (2015).
37. T. Qiu1, S. Palagi1, A. G. Mark1, K. Melde1, F. Adams and P. Fischer, *Appl. Phys. Lett.*, **109**, 191602 (2016).
38. L. Ren, N. Nama, J. M. McNeill, F. Soto, Z. Yan, W. Liu, W. Wang, J. Wang and T. E. Mallouk, *Sci. Adv.*, **5**, eaax3084 (2019).
39. F. W. Liu, Y. Zhan and S. K. Cho, *J. Micromech. Microeng.*, **31**, 084001 (2021).